Is Image Super-resolution Helpful for Other Vision Tasks?

Dengxin Dai* Yujian Wang* Yuhua Chen Luc Van Gool
Computer Vision Lab, ETH Zurich
{dai, yuhua.chen, vangool}@vision.ee.ethz.ch, yjwang@student.ethz.ch

Abstract

Despite the great advances made in the field of image super-resolution (ISR) during the last years, the performance has merely been evaluated perceptually. Thus, it is still unclear whether ISR is helpful for other vision tasks. In this paper, we present the first comprehensive study and analysis of the usefulness of ISR for other vision applications. In particular, six ISR methods are evaluated on four popular vision tasks, namely edge detection, semantic image segmentation, digit recognition, and scene recognition. We show that applying ISR to input images of other vision systems does improve their performance when the input images are of low-resolution. We also study the correlation between four standard perceptual evaluation criteria (namely PSNR, SSIM, IFC, and NQM) and the usefulness of ISR to the vision tasks. Experiments show that they correlate well with each other in general, but perceptual criteria are still not accurate enough to be used as full proxies for the usefulness. We hope this work will inspire the community to evaluate ISR methods also in real vision applications, and to adopt ISR as a pre-processing step of other vision tasks if the resolution of their input images is low.

1. Introduction

Image super-resolution (ISR) aims to sharpen smooth rough edges and enrich missing textures in images that have been enlarged using a general up-scaling process (such as a bilinear or bicubic process), thereby delivering an image with high-quality resolution [13, 46, 48, 38, 10, 6]. ISR systems can be used to adapt images to displaying devices of different dimensions, to map image textures to 2D/3D shapes, and to deliver pleasing visualization for data that are inherently low-resolution such as image or videos from surveillance cameras. Despite the popularity of ISR in the past years, their performance has merely been evaluated perceptually and/or by evaluation criteria reflecting perceptual quality such as PSNR and SSIM. Therefore, it is still unclear whether ISR is helpful in general to other vision tasks and whether the perceptual criteria are able to reflect the usefulness. This paper answers the questions.

We here present reasons why ISR can be helpful for other vision tasks, in addition to improving perceptual quality. As we know, most of current vision systems consist in two phases: training and testing. Although features have been designed to overcome the influence of scale changes, it is still a blessing if 1) the training and testing images are of the same/similar resolution; and/or 2) input images can be converted to the resolution at which the features and the models were designed. It happens quite common that training and testing data are of different resolutions, *e.g*. training images are from expensive sensors while testing images from cheap ones. If testing images are of higher resolution, downsampling them with linear filters does the job. If the opposite holds, however, sophisticated ISR methods are required to super-resolve the testing images. Also, vision systems are often designed and optimized (*e.g*. the features) for images of the most 'popular' resolution at the time. ISR is useful to super-resolve images which are of lower-resolution than the images for which the features and models are designed and learned. One example is object recognition with surveillance cameras: popular features [23, 9, 28] for object recognition are designed for normal images which are of higher-resolution than surveillance scenes in general. For this case, even the training data and testing data are of the same resolution, ISR is still helpful by enabling feature extraction at an appropriate resolution.

In order to sufficiently sample the space of ISR methods and potential vision tasks, six ISR methods are chosen and evaluated on four popular vision applications. The ISR methods are Zeyde *et al*. [48], ANR [38], A+ [39], SRCNN [10], JOR [6], and SRF [31]. They are chosen because 1) they are popular and representative; 2) they have code available; and 3) they are computationally efficient. The four vision applications include image boundary detection, semantic image segmentation, digit recognition, and scene recognition. The tasks are chosen because they are representatives of current low- and high-level vision tasks. The data of digits is chosen because low-resolution inputs

*Joint first author

are very likely to occur in this field. For all the tasks, we apply standard approaches with varying modes of the input images: from low-resolution images, to super-resolved images by the six ISR methods, and to the high-resolution images. The experimental results suggest that ISR is helpful for these vision tasks if the resolution of the input images are low, and that the standard evaluation criteria, including PSNR, SSIM, IFC, and NQM, correlate generally well with the usefulness of ISR methods, but should not be used as the full proxies of the usefulness if high precision is required.

The paper is organized as follows. Section 2 reports related work. Evaluation on the four vision tasks are conducted in Section 3.1 to Section 3.4. Finally, the paper concludes in Section 4.

2. Related Work

There is a large body of work addressing image super-resolution task. We breifly summarize them. The oldest direction is represented by variants of interpolation, such as Bilinear and Bicubic [11, 37]. They represent the simplest and the most popular methods. However, they often produce visual artifacts such as blurring, ringing, and blocking, which follows the fact that their assumptions of smoothness and band-limited image data hardly hold in real cases. Due to these reasons, more realistic priors and regularization have been developed, such as the sparse derivative priors in [36], the PDE-based regularization in [41], the edge smoothness prior in [8], and gradient profile [34]. Despite the improvement by these methods, the explicit forms of prior are still insufficient to express the richness of real-world image data.

In recent years, example-based image super-resolution has raised the most attention due to its good performance and simplicity. In this stream, the task is to learn a mapping function from a collection of LR images and their corresponding high-resolution (HR) ones. The LR and HR data can be collected from the test image itself or from an external dataset. Methods [12, 14, 43, 17] in the former stream draw on the 'self-similarity' of images across scales, and have obtained great success. However, they are normally relatively slow because on-line learning is needed for the dictionary. Methods in the latter group rely on extra training data, unleashing the learning capacity of many learning methods. The KNN method [13] and its variants [1, 45, 6, 4] have gained great attention. More sophisticated learning methods such as Sparse Coding [46, 20, 38, 39, 42], SVM [27], Random Forests [31, 30, 29], and Deep Neural Network [10, 3, 42] have been applied widely to the task as well. One exceptional work is [35], using scene matching with internet images for image super-resolution. Since example-based methods with extra training data obtain state-of-the-art performance for ISR, our evaluation is focused mostly on this stream.

There is also a survey paper on ISR [25], providing an excellent summary of the theory and applications of ISR. [40] exploits seven ways to improve the performance of general example-based ISR methods. The work most relevant to ours is [44], where different ISR methods are evaluated. While sharing similarities, the two methods still differ significantly. [44] conducted user studies for perceptual evaluation, solely with visual comparison and under evaluation criteria such as PSNR and SSIM. Our work, however, integrates ISR methods into systems of other vision applications and evaluates the usefulness of ISR to these vision tasks. There are also works employing ISR to improve the quality (resolution) of the input images of other vision algorithms, such as [16] for face recognition and [19] for pedestrian identification. However, these tasks are specific and the ISR methods used are highly specialized. Our work, however, evaluates general ISR methods with a variety of popular vision tasks.

3. Evaluation

In this section, we briefly describe the six ISR methods: Zeyde *et al.* [48], ANR [38], A+ [39], SRCNN [10], JOR [6], and SRF [31], followed by the evaluation on the four vision tasks. The six methods, starting out with the results of Bicubic interpolation, learn from examples to recover the missing high-frequency parts. As to the examples, the six methods are all trained with the same training dataset from [46], which consists of 91 images of flowers, faces, *et al.* For implementation, we use the codes provided by the authors. Readers are referred to their papers for details. As to scaling factors, we evaluate with ×3 and ×4, which are commonly used in previous papers.

For datasets, we use the standard ones for the four vision tasks, though not the most challenging ones. To generate inputs for our evaluation, we downscale the original images of the datasets by factors ×3 and ×4 to create the low-resolution (LR) images and then upscale them by each of the six ISR methods to the resolution of the original images, which are then used as the inputs for the vision tasks. The standard approaches to the four tasks are then applied to all the six super-resolved versions of the images. The corresponding performances are recorded to evaluate the usefulness of the ISR methods for the vision tasks, with a comparison to Bicubic Interpolation, and the original images. We also evaluate the ISR methods on these datasets with four standard perceptual criteria [44], namely PSNR, SSIM, IFC, and NQM, in order to see their correlation to the usefulness of ISR to these vision tasks.

3.1. Boundary Detection

Boundary Detection (BD) is a very popular low-level vision task and serves as a crucial component for many high-level vision systems [24, 18]. This section evaluates the

BSDS300		Bicubic	Zeyde *et al.* [48]	ANR[38]	SRCNN[10]	A+[39]	JOR[6]	SRF[31]	Original
×**3**	PSNR	27.15	27.87	27.88	28.10	**28.18**	28.17	28.17	—
	SSIM	0.736	0.770	0.773	0.777	**0.781**	**0.781**	0.780	—
	IFC	2.742	3.203	3.248	3.131	**3.374**	3.360	3.366	—
	NQM	27.42	31.80	31.95	31.28	32.35	**32.41**	32.40	—
	AUC	0.647	**0.675**	0.665	0.668	**0.675**	0.674	0.674	0.696
×**4**	PSNR	25.92	26.51	26.51	26.66	**26.77**	26.74	26.74	—
	SSIM	0.667	0.697	0.699	0.702	**0.709**	0.707	0.707	—
	IFC	1.839	2.195	2.231	2.117	**2.325**	2.316	2.293	—
	NQM	21.15	24.30	24.37	24.19	**24.98**	24.96	**24.98**	—
	AUC	0.595	0.647	0.635	0.650	**0.656**	0.655	0.652	0.696

Table 1. Average PSNR, SSIM, IFC, NQM values of ISR methods on BSDS300 and average AUC values of boundary detection via CBD [18] on the super-resolved images by the ISR methods and the original images. The best one is shown in **bold** and the second best underlined.

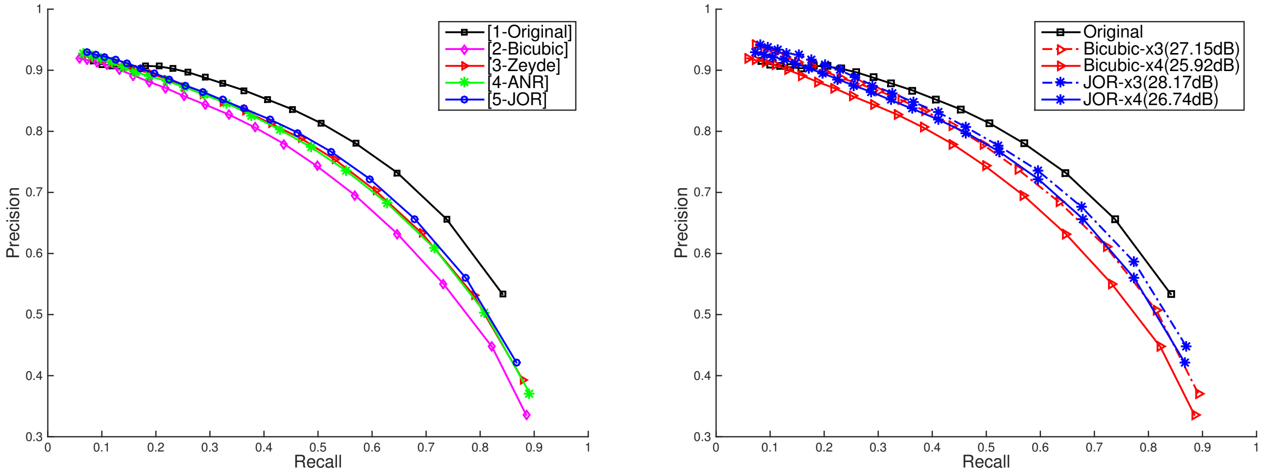

(a) PR curves with scaling factor x4

(b) PR curves with scaling factor x3 and x4

Figure 1. Average PR curves of boundary detection via CBD [18] on the super-resolved images by some of the five ISR methods and on the original images of BSDS300. (a) curves for scaling factor x4, where SRCNN and A+ are not shown for visual clarity as they are very similar to JOR. (b) a comparison of scaling factor x3 and x4, where only Bicubic Interpolation and JOR are shown for visual clarity.

usefulness of ISR methods for BD. We use Crisp Boundary Detection [18] (CBD), which is an unsupervised algorithm, deriving an affinity measure with point-wise mutual information between pixels and utilizing this affinity with spectral clustering method to detect boundaries. It produces pixel-level boundaries and achieves state-of-art results. The performances are evaluated on the BSDS300 dataset [24]. The whole dataset consists of 300 images (200 for training and 100 for testing) along with human annotations. The quality of detected boundaries is evaluated by precision-recall (PR) curves, following Berkeley Benchmark [24].

Table 1 lists the AUC values of BD on the eight sets of images, along with the values of PSNR, SSIM, IFC, and NQM of corresponding ISR methods. Fig. 1 shows the average PR curves. From the table and the figure, it can be observed that ISR methods do improve, over simple interpolation, the performance of BD when input images are of low-resolution. For instance, JOR improves the AUC by 0.06 when factor x4 is considered. This is because ISR methods perform better in increasing the resolution of the LR images to the resolution for which the BD method (CBD [18] in this case) was designed. CBD uses highly localized features to predict pixel-level boundaries, whose accuracy is affected largely by the recovered details locally. As a result, the six learning-based ISR methods all perform better than Bicubic Interpolation. This suggests that ISR should be considered as a pre-processing step for BD if the input images are of LR. One may argue that adapting or re-training the BD method may increase its performance for LR images. It is true, but we have to admit that adapting or re-training the approach requites expertise of BD and deep understanding of the approach used. Enhancing the resolution of LR inputs, however, is much more straightforward for general practitioners, especially given the fact that BD is just one of

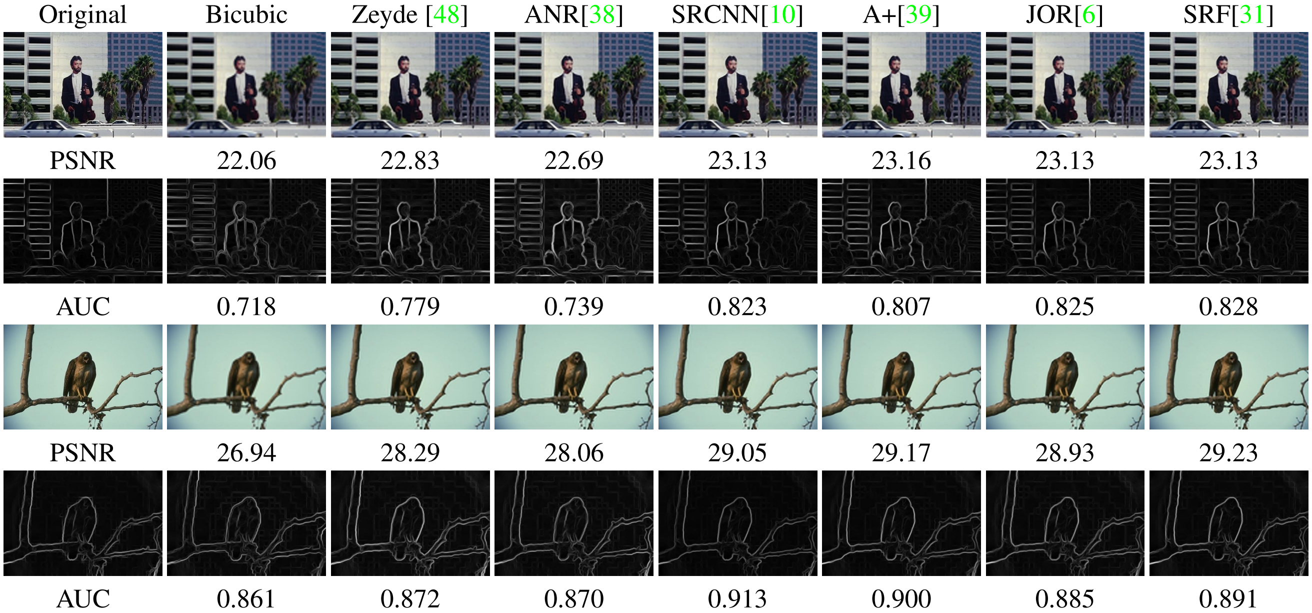

Figure 2. Super-resolved examples with their PSNR values and corresponding detected boundary maps by CBD [18] with their AUC values. Better seen on the screen.

such examples as shown in following sections.

It can also be found that the four standard perceptual criteria correlate quite well with the usefulness of ISR methods for the task of BD. ISR methods which yield better perceptual quality (based on the four perceptual criteria) often obtain better boundary detection results. However, perceptual criteria should not be considered as full proxies for the usefulness of ISR methods to BD. For instance, SRCNN outscores A+ in terms of PSNR while having a lower AUC value, when factor ×3 is used. This suggests that measuring the usefulness of ISR methods for BD directly in a real system is necessary if a high precision is requited. In general, SRCNN, A+, JOR and SRF are among the most useful ISR methods for the task of BD for the dataset and approach considered. The third finding from the table and figure is that ISR methods are more useful when the scaling factor is larger, which means they are more needed when the input images are of very low-resolution.

In Fig. 2, we show visual examples, with the super-resolution results and their corresponding BD results. From the figure, it is evident that example-based ISR methods improve the quality of BD results with sharper true boundaries and fewer spurious ones. However, there is still a large room for improvement as the OB results on the super-resolved images by the ISR methods are still substantially worse than the result on the original ('HR') image.

3.2. Semantic Image Segmentation

In this section, we consider the task of semantic image segmentation, which aims to assign a semantic label to each pixel of the image, such as *tree*, *road*, and *car*. It is a very popular high-level vision task with a large number of methods proposed [33, 15, 22]. We follow the footsteps of most previous works on semantic image segmentation and choose the standard MSRC-21 [32] dataset for the evaluation. MSRC-21 consists of 591 images of 21 semantic categories. For the segmentation method, we employ the recent approach [15] for its simplicity in order to better show the influence of ISR. [15] presents a fast approximate nearest neighbor algorithm for image labeling. They build a super-pixel graph from annotated set of training images. At test time, they transfer labels from the training images to the test image via matching super-pixels in the graph. The distance between super-pixels in the feature space is approximated by edge distance in the super-pixel graph where the edge weights are learned from the training set. This method shows comparable results to the state-of-the-art methods. For the implementation, we use the authors' code with the default settings.

In order to evaluate the ISR methods for semantic image segmentation, we train the method [15] with the original training images (*e.g.* the HR images) and test the trained model on eight versions of the testing images, created by down-sampling the original images and then up-solving them by the ISR methods to the resolution of the original images. Again, the performance is tested for scaling factor x3 and x4. Table 2 lists the results of all ISR methods, where the average precision over pixels (APP) and the average precision over classes (APC) are reported, along with the values of the four perceptual criteria. As we can see from the table, all the six ISR methods yield significantly better results than Bicubic Interpolation. Putting it into an-

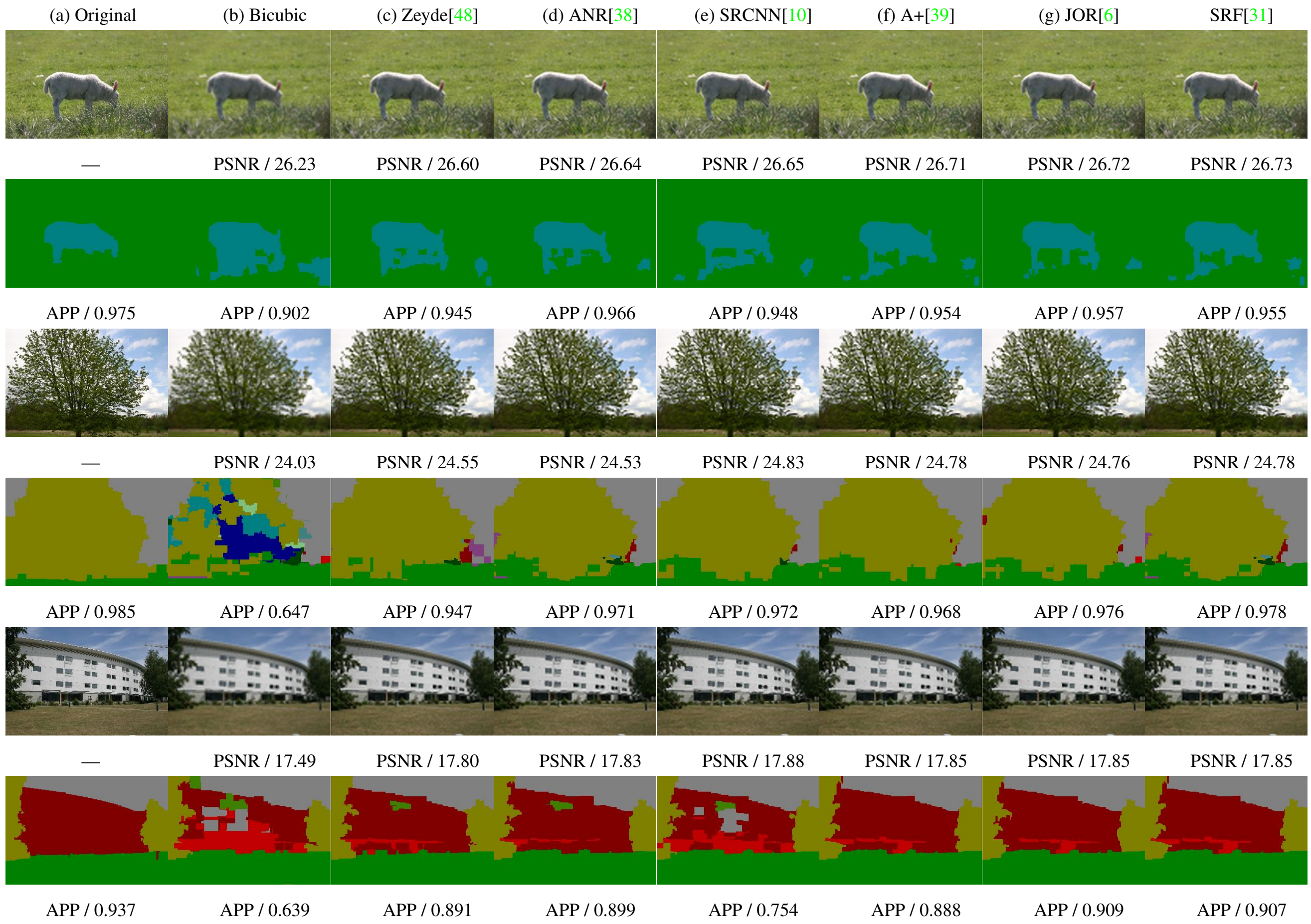

Figure 3. Examples for semantic image segmentation: super-resolved images with their PSNR values and the corresponding labeling results with their average precision over pixels (APP) are shown. Better seen on the screen.

Table 2. Average PSNR, SSIM, IFC, NQM, and labeling accuracy on MSRC-21 dataset, where APP indicates Average Precision over Pixels, and APC means Average Precision over Classes. The best performance is shown in **bold** and the second best is underlined.

MSRC-21		Bicubic	Zeyde *et al.* [48]	ANR[38]	SRCNN[10]	A+[39]	JOR[6]	SRF[31]	Original
×**3**	PSNR	25.29	26.02	26.00	26.21	26.28	26.28	**26.35**	—
	SSIM	0.689	0.726	0.728	0.733	0.737	0.737	**0.738**	—
	IFC	2.677	3.214	3.250	3.131	3.390	3.396	**3.640**	—
	NQM	19.56	22.48	22.47	22.64	23.10	23.16	**23.20**	—
	APP	0.692	0.762	0.770	0.777	0.780	**0.783**	0.782	0.844
	APC	0.592	0.662	0.674	0.681	0.684	**0.687**	0.685	0.743
×**4**	PSNR	24.04	24.65	24.63	24.77	24.88	24.86	**24.90**	—
	SSIM	0.608	0.641	0.643	0.646	0.654	0.652	**0.660**	—
	IFC	1.694	2.043	2.066	1.992	2.171	2.151	**2.301**	—
	NQM	14.75	16.56	16.55	16.73	17.10	**17.12**	16.99	—
	APP	0.582	0.665	0.677	0.673	**0.682**	0.674	0.674	0.844
	APC	0.505	0.569	0.584	0.588	0.591	0.586	**0.605**	0.743

other way, these learning-based super-resolution systems, in addition to improving visual quality of LR images, do facilitate semantic labeling tasks and improve the performance substantially when the resolution of the testing images are lower than that of the training images. The results suggest that it is worth effort to integrate ISR methods into real image labeling systems if the resolutions of training and testing images are distinctive. This is highly probably the case for real semantic labeling systems where training images on the server side are from expensive sensors and testing im-

SVHN		Bicubic	Zeyde *et al.* [48]	ANR[38]	SRCNN[10]	A+[39]	JOR[6]	SRF[31]	Original
×3	PSNR	33.39	35.40	**35.73**	35.03	34.85	34.90	34.82	—
	SSIM	0.912	0.946	**0.949**	0.946	0.946	0.948	0.948	—
	IFC	2.050	2.331	**2.417**	2.291	2.389	2.346	2.355	—
	NQM	10.23	12.59	**12.91**	12.16	12.17	12.21	12.19	—
	Accuracy	0.766	0.774	0.777	**0.779**	0.778	0.775	0.778	0.793
×3[R]	PNSR	33.39	36.30	36.53	35.99	37.20	**37.26**	37.12	—
	SSIM	0.912	0.951	0.953	0.947	0.963	**0.964**	0.963	—
	IFC	2.050	2.484	2.550	2.427	2.726	**2.730**	2.701	—
	NQM	10.23	13.30	13.53	13.04	14.24	**14.25**	14.17	—
	Accuracy	0.766	0.775	0.774	0.773	0.783	**0.786**	0.778	0.793
×4	PSNR	29.08	30.63	30.72	**30.83**	30.45	30.47	30.11	—
	SSIM	0.787	0.842	0.847	0.849	0.847	**0.850**	0.845	—
	IFC	1.262	1.352	1.367	**1.368**	1.365	1.339	1.287	—
	NQM	6.211	7.864	7.978	**8.021**	7.732	7.720	7.453	—
	Accuracy	0.712	0.731	0.731	0.730	**0.737**	0.722	0.729	0.795
×4[R]	PNSR	29.08	31.07	31.06	31.00	**32.00**	31.71	31.77	—
	SSIM	0.787	0.858	0.862	0.856	**0.887**	**0.887**	0.886	—
	IFC	1.262	1.456	1.466	1.427	**1.639**	1.599	1.589	—
	NQM	6.211	8.268	8.286	8.209	**9.162**	8.872	8.962	—
	Accuracy	0.712	0.735	0.730	0.732	0.744	0.744	**0.749**	0.795

Table 3. Results of digit recognition on the SVHN dataset. The k-NN classifier is trained and applied on HOG features of each pair of super-resolved training and test sets. Methods marked with [R] are retrained using the unused digits of the SVHN dataset. The best performance is shown in **bold** and the second best is underlined.

ages on the user side are from cheap sensors such as cameras of an mobile phone. Another observation from the table is that the standard perceptual evaluation criteria correlate quite well with the usefulness of ISR methods for semantic image segmentation. This implies that good visual quality also facilitates computer systems for recognition. This can ascribed to the fact that the semantics are defined by human and computer are trained to conduct a human vision task which is of course very relevant to the perceptual quality of images. Also, ISR methods are more useful when the scaling factor is larger, which means they are more needed when the input images are of very low-resolution. The observation is consistent with the one we had for BD in Sec. 3.1.

In Fig. 3, we show three image examples, with the super-resolution results and their corresponding labeling results. From the figure, it is evident that ISR methods improve the quality of the labeling results. For instance, in the third example, results of Bicubic Interpolation labeled a large area of the building to sky, which is probably due to the detailed textures on the building are missing in the interpolated image. The missing texture are recovered (to some extend) by the example-based ISR methods, leading to better labeling results. Also, it can be found that RGB images that have small difference in perception may lead to totally different labeling results, e.g. the tree in the second example. This implies that there is still room for computer recognition systems to improve in order to be as robust as human vision.

3.3. Digit Recognition

In this section, we test the usefulness of ISR methods for the task of digit recognition where the training images and the test image are both of low-resolution. We use the Street View House Numbers (SVHN) [26] dataset which contains more than 100,000 images of house numbers obtained from Google Street View. Each image presents a single digit at its center and has the same size of 32×32 pixels. We select 26,032 and 10,000 images from the dataset as our training and test set. In order to evaluate the usefulness of ISR methods for digit recognition, we here down-sample all the images by factor x3 and factor x4, and up-sample the down-sampled images to the resolution of the original images by the ISR methods. As the SVHN dataset merely presents numbers from 0 to 9, it is highly specific and quite different from the training dataset from [46] that is used to train the ISR methods. Therefore, we re-trained all ISR methods with the unused images from the SVHN dataset, to study the generality of ISR methods. After adding the re-trained methods, we now have twelve datasets of super-resolved results, one dataset from Bicubic Interpolation and one dataset of the original images. As to the classifier, we use the k-NN with $k = 5$ for each of the eight image sets with HOG feature [9] as input. Other values of k yield a similar trend.

The classification performance is listed in Table 3. The table demonstrates that ISR methods do improve the perfor-

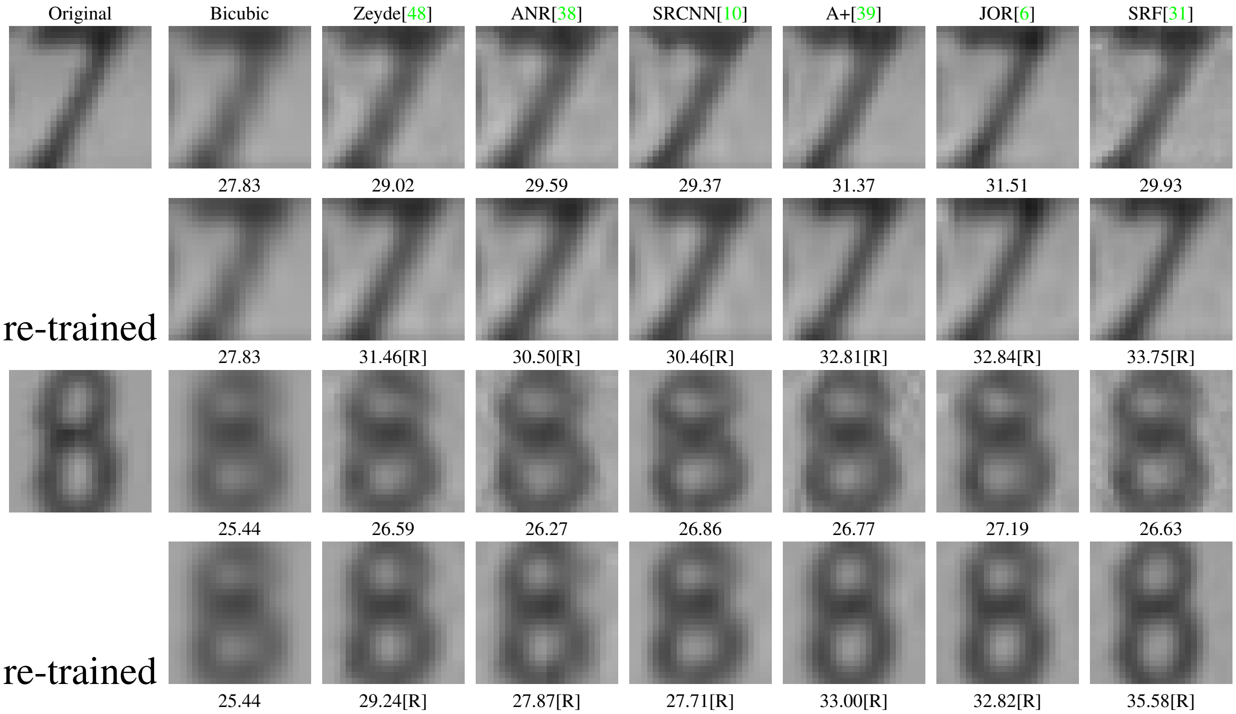

Figure 4. Super-resolved results and corresponding PSNR values of two digits. Methods marked with [R] are retrained using the unused digits of the SVHN dataset. Better seen on the screen.

mance of digit recognition over simple interpolation, and that the four perceptual criteria correlate quite well with the usefulness of ISR methods for digit recognition. The reason of the improvement is that HOG feature was designed for images of normal resolution, so by applying ISR methods to the LR input images, HOG can be extracted from images of suitable resolution. However, we find that with the standard, general training dataset [46], Zeyde et al. and ANR perform better than SRCNN, A+ , JOR and SRF, which is different from the results of the previous two tasks with general images. This observation suggests that Zeyde et al. and ANR are more generally applied than the other four state-of-the-art ISR methods. One possible reason is that models of higher complexity are more likely to overfit to the training data. The problem can be solved by re-training the model with data of similar distribution as the test data. We re-trained all the six method with unlabeled digits in SVHN, and as expected the performance is improved significantly, according to the four perceptual criteria or recognition accuracy. See Table 3 for the improvement. After re-training, the four methods SRCNN, A+, JOR, and SRF yield the best results. In Fig. 4, we show two digits, along with their super-resolved results by factor x3 and the PSNR values. From the figure, it is clear to see the artifacts generated by the ISR methods trained with general training data. The introduced artifacts lead to noisy HOG features, which in turn confuse the classifier. All the evidence leads to conclusions similar to that drawn for boundary detection and semantic image segmentation: (1) ISR methods are generally helpful for recognizing digits of low-resolution; and (2) perceptual evaluation criteria reflect the usefulness of ISR to digit recognition quite well. In addition, we find that the performance of ISR methods will improve significantly if they are re-trained with domain specific data.

3.4. Scene Recognition

In this section, we evaluated six ISR methods on the task of scene recognition. We tested the methods on the Scene-15 dataset [21], which has been widely used for image classification and clustering [21, 5, 7]. Scene-15 contains 15 scene categories in both indoor and outdoor environments. Each category has 200 to 400 images, and they are of size 300 × 250 pixels on average. We use the same experimental designs as for the previous tasks: down-sampling all the images by factor x3 and factor x4, and up-sampling the down-sampled images to the resolution of the original images by the six ISR methods, thus resulting in six super-resolved datasets for each scaling factor, one for bicubic interpolation, and one for the original (HR) images. As to the features, we use the Convolutional Neural Network (CNN) features [2], obtained from an off-the-shelf CNN model pre-trained on the ImageNet. The feature is chosen as CNN feature has achieved state-of-the-art performance for image classification [2]. It is worth noticing that the training and

Scene-15		Bicubic	Zeyde [48]	ANR[38]	SRCNN[10]	A+[39]	JOR[6]	SRF [31]	Original
×3	PSNR	25.12	25.85	25.87	26.10	**26.19**	26.18	26.13	—
	SSIM	0.73	0.78	0.77	0.78	0.79	0.79	**0.80**	—
	IFC	2.82	3.34	3.43	3.20	3.58	**3.60**	3.58	—
	NQM	19.75	22.69	22.73	22.81	23.39	**23.43**	23.30	—
	Accuracy	0.770	0.777	0.777	0.780	**0.782**	**0.782**	0.778	0.809
×4	PSNR	24.32	24.99	24.95	25.06	**25.24**	25.22	25.19	—
	SSIM	0.674	0.701	0.702	0.704	0.720	0.719	**0.722**	—
	IFC	1.597	1.923	1.911	1.806	**2.021**	2.010	2.014	—
	NQM	14.43	16.12	16.05	16.07	**16.62**	16.61	16.57	—
	Accuracy	0.735	0.752	0.753	0.748	**0.754**	0.753	0.753	0.809

Table 4. Average PSNR, SSIM, IFC, NQM values and the accuracy of scene recognition on Scene-15 dataset.

testing data are processed the same way, *i.e*. down-sampled by bicubic interpolation and up-sampled by the same ISR method (one of the six). The convolutional results at layer 16 were stacked as the CNN feature vector, with dimensionality of 4096. As to the classification, we use 15 images per class as the training samples, and the rest left for testing.

The classification accuracies over 10 random training-testing splits are averaged and reported in Table 4, along with the results according to the four perceptual criteria. The table shows that learning-based ISR methods are helpful for scene recognition with the deep neural network when the input images are of low-resolution. The four perceptual criteria also correlate generally well with usefulness of ISR methods for this task, which is in line with the conclusions drawn for previous vision tasks. Images at multiple scales have recently been employed for training deep neural networks [47, 22], and they show improvement over a single scale. It is interesting to see how ISR methods help to generate multiple scales of the input images to train better neural networks. We leave this as our future work.

4. Discussion and Conclusion

We have evaluated the usefulness of image super-resolution (ISR) for a variety of different vision tasks. Six ISR methods have been employed and evaluated on four popular vision tasks. Three general conclusions can be drawn from experiments on the four tasks: 1) ISR methods are helpful in general for other vision tasks when the resolution of input images are low; 2) standard perceptual criteria, namely PSNR, SSIM, IFC, NQM, correlate quite well with the usefulness of ISR methods for the vision tasks, but they are not accurate enough to be used as full proxies; and 3) even with the state-of-the-art ISR methods, the performance with the super-resolved images are still significantly inferior to that with the original, high-resolution images.

Although it is generally believed that ISR methods is helpful for other vision tasks, this work has formalized the common conception and conducted quantitative evaluation. We hope this work will be an inspiration for the community to integrate ISR methods into other vision systems when the input images are of low-resolution or when multiple resolutions are needed, and to evaluate ISR methods in real vision tasks, in addition to merely inspecting the visual quality. The work may inspire the community to design super-resolution algorithm for specific vision task rather than merely levering the perceptual criteria.

We acknowledge that for some tasks, the approaches and the datasets do not represent the state of the arts. However, they are standard ones and we believe they are sufficient to support the conclusions. Method evaluation on more vision tasks with more challenging datasets, testing multiple approaches for the same task, and testing different parameter settings for the same approach constitute our future work. The code and data of this work are available at `www.vision.ee.ethz.ch/~daid/SR4VisionTask`.

Acknoledgements The work is supported by the ERC Advanced Grant Varcity (#273940).

References

[1] H. Chang, D.-Y. Yeung, and Y. Xiong. Super-resolution through neighbor embedding. *CVPR*, 2004. 2

[2] K. Chatfield, K. Simonyan, A. Vedaldi, and A. Zisserman. Return of the devil in the details: Delving deep into convolutional nets. In *BMVC*, 2014. 7

[3] Z. Cui, H. Chang, S. Shan, B. Zhong, and X. Chen. Deep network cascade for image super-resolution. In *ECCV*. 2014. 2

[4] D. Dai, T. Kroeger, R. Timofte, and L. Van Gool. Metric imitation by manifold transfer for efficient vision applications. In *CVPR*, 2015. 2

[5] D. Dai, M. Prasad, C. Leistner, and L. V. Gool. Ensemble partitioning for unsupervised image categorization. In *ECCV*, 2012. 7

[6] D. Dai, R. Timofte, and L. Van Gool. Jointly optimized regressors for image super-resolution. In *Eurographics*, 2015. 1, 2, 3, 4, 5, 6, 7, 8

[7] D. Dai and L. Van Gool. Ensemble projection for semi-supervised image classification. In *ICCV*, 2013. 7

[8] S. Dai, M. Han, W. Xu, Y. Wu, and Y. Gong. Soft edge smoothness prior for alpha channel super resolution. In *CVPR*, 2007. 2

[9] N. Dalal and B. Triggs. Histograms of oriented gradients for human detection. *CVPR*, 1, 2005. 1, 6

[10] C. Dong, C. C. Loy, K. He, and X. Tang. Learning a deep convolutional network for image super-resolution. In *ECCV*, 2014. 1, 2, 3, 4, 5, 6, 7, 8

[11] C. E. Duchon. Lanczos Filtering in One and Two Dimensions. *J. Appl. Meteorology*, 18:1016–1022, 1979. 2

[12] G. Freedman and R. Fattal. Image and video upscaling from local self-examples. *ACM Trans. Graph.*, 30(2):12:1–12:11, Apr. 2011. 2

[13] W. T. Freeman, T. R. Jones, and E. C. Pasztor. Example-based super-resolution. *IEEE Computer Graphics and Applications*, 22(2):56–65, 2002. 1, 2

[14] D. Glasner, S. Bagon, and M. Irani. Super-resolution from a single image. In *ICCV*, 2009. 2

[15] S. Gould, J. Zhao, X. He, and Y. Zhang. Superpixel graph label transfer with learned distance metric. In *ECCV 2014*. 2014. 4

[16] P. Hennings-Yeomans, S. Baker, and B. V. Kumar. Simultaneous super-resolution and feature extraction for recognition of low resolution faces. In *CVPR*, 2008. 2

[17] J.-B. Huang, A. Singh, and N. Ahuja. Single image super-resolution from transformed self-exemplars. In *CVPR*, 2015. 2

[18] P. Isola, D. Zoran, D. Krishnan, and E. H. Adelson. Crisp boundary detection using pointwise mutual information. In *ECCV*. 2014. 2, 3, 4

[19] X.-Y. Jing, X. Zhu, F. Wu, X. You, Q. Liu, D. Yue, R. Hu, and B. Xu. Super-resolution person re-identification with semi-coupled low-rank discriminant dictionary learning. In *CVPR*, 2015. 2

[20] K. I. Kim and Y. Kwon. Single-image super-resolution using sparse regression and natural image prior. *PAMI*, 32(6):1127–1133, 2010. 2

[21] S. Lazebnik, C. Schmid, and J. Ponce. Beyond bags of features: Spatial pyramid matching for recognizing natural scene categories. In *CVPR*, 2006. 7

[22] J. Long, E. Shelhamer, and T. Darrell. Fully convolutional networks for semantic segmentation. In *CVPR*, 2014. 4, 8

[23] D. G. Lowe. Distinctive image features from scale-invariant keypoints. *IJCV*, 60(2):91–110, 2004. 1

[24] D. Martin, C. Fowlkes, D. Tal, and J. Malik. A database of human segmented natural images and its application to evaluating segmentation algorithms and measuring ecological statistics. In *ICCV*, 2001. 2, 3

[25] K. Nasrollahi and T. B. Moeslund. Super-resolution: a comprehensive survey. *Machine Vision and Applications*, 25(6):1423–1468, 2014. 2

[26] Y. Netzer, T. Wang, A. Coates, A. Bissacco, B. Wu, and A. Y. Ng. Reading digits in natural images with unsupervised feature learning. In *NIPS Workshop*, 2011. 6

[27] K. Ni and T. Nguyen. Image superresolution using support vector regression. *Image Processing, IEEE Transactions on*, 16(6):1596–1610, 2007. 2

[28] A. S. Razavian, H. Azizpour, J. Sullivan, and S. Carlsson. Cnn features off-the-shelf: An astounding baseline for recognition. In *CVPR Workshop*, 2014. 1

[29] G. Riegler, S. Schulter, M. Rüther, and H. Bischof. Conditioned regression models for non-blind single image super-resolution. In *ICCV*, 2015. 2

[30] J. Salvador and E. Perez-Pellitero. Naive bayes super-resolution forest. In *ICCV*, 2015. 2

[31] S. Schulter, C. Leistner, and H. Bischof. Fast and accurate image upscaling with super-resolution forests. In *CVPR*, 2015. 1, 2, 3, 4, 5, 6, 7, 8

[32] J. Shotton, J. Winn, C. Rother, and A. Criminisi. Textonboost: Joint appearance, shape and context modeling for multi-class object recognition and segmentation. In *ECCV*, 2006. 4

[33] M. C. R. R. C. T. C. K. Shotton, J.; Johnson. Semantic texton forests for image categorization and segmentation. In *CVPR*, 2008. 4

[34] J. Sun, Z. Xu, and H.-Y. Shum. Image super-resolution using gradient profile prior. In *CVPR*, 2008. 2

[35] L. Sun and J. Hays. Super-resolution from internet-scale scene matching. In *ICCP*, 2012. 2

[36] M. F. Tappen, B. C. Russell, and W. T. Freeman. Exploiting the sparse derivative prior for super-resolution and image demosaicing. In *In IEEE Workshop on Statistical and Computational Theories of Vision*, 2003. 2

[37] P. Thévenaz, T. Blu, and M. Unser. *Image interpolation and resampling*. 2000. 2

[38] R. Timofte, V. De Smet, and L. Van Gool. Anchored neighborhood regression for fast example-based super resolution. In *ICCV*, 2013. 1, 2, 3, 4, 5, 6, 7, 8

[39] R. Timofte, V. De Smet, and L. Van Gool. A+: Adjusted anchored neighborhood regression for fast super-resolution. In *ACCV*, 2014. 1, 2, 3, 4, 5, 6, 7, 8

[40] R. Timofte, R. Rothe, and L. Van Gool. Seven ways to improve example-based single image super resolution. *arXiv:1511.02228*, 2015. 2

[41] D. Tschumperle and R. Deriche. Vector-valued image regularization with pdes: a common framework for different applications. *PAMI*, 27(4):506–517, 2005. 2

[42] Z. Wang, D. Liu, J. Yang, W. Han, and T. Huang. Deeply improved sparse coding for image super-resolution. In *ICCV*, 2015. 2

[43] C.-Y. Yang, J.-B. Huang, and M.-H. Yang. Exploiting self-similarities for single frame super-resolution. In *ACCV*. 2011. 2

[44] C.-Y. Yang, C. Ma, and M.-H. Yang. Single-image super-resolution: A benchmark. In *ECCV*. 2014. 2

[45] C.-Y. Yang and M.-H. Yang. Fast direct super-resolution by simple functions. In *ICCV*, 2013. 2

[46] J. Yang, J. Wright, T. Huang, and Y. Ma. Image super-resolution via sparse representation. *Image Processing, IEEE Transactions on*, 19(11):2861–2873, 2010. 1, 2, 6, 7

[47] D. Yoo, S. Park, J.-Y. Lee, and I. S. Kweon. Multi-scale pyramid pooling for deep convolutional representation. In *CVPR Workshop*, 2015. 8

[48] R. Zeyde, M. Elad, and M. Protter. On single image scale-up using sparse-representations. In *Curves and Surfaces*, pages 711–730, 2012. 1, 2, 3, 4, 5, 6, 7, 8